The Influence of Chemical Bonding Configuration on Atomic Identification by Force Spectroscopy

Joachim Welker, Alfred John Weymouth, and Franz J. Giessibl*

Institute of Experimental and Applied Physics, Experimental Nanoscience, University of Regensburg, Universitaetsstrasse 31, 93053 Regensburg, Germany

ABSTRACT

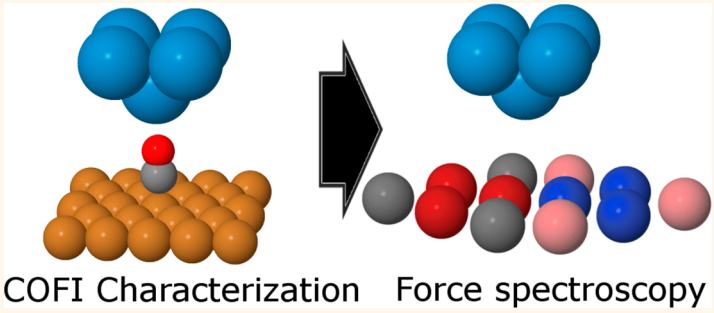

The force between two atoms depends not only on their chemical species and distance, but also on the configuration of their chemical bonds to other atoms. This strongly affects atomic force spectroscopy, in which the force between the tip of an atomic force microscope and a sample is measured as a function of distance. We show that the short-range forces between tip and sample atoms depend strongly on the configuration of the tip, to the point of preventing atom identification with a poorly defined tip. Our solution is to control the tip apex before using it for spectroscopy. We demonstrate a method by which a CO molecule on Cu can be used to characterize the tip. In combination with gentle pokes, this can be used to engineer a specific tip apex. This CO Front atom Identification (COFI) method allows us to use a well-defined tip to conduct force spectroscopy.

KEYWORDS: atomic force microscopy · chemical identification · atomic forces

Non-Contact Atomic Force Microscopy (NC-AFM) has become an analytical tool for surface chemistry.[1] One focus of this development is the discrimination of different atoms to the point of distinguishing the same atomic species in different local environments.[2] Sugimoto *et al.*[3] demonstrated that NC-AFM could identify three atomic species (Si, Pb, and Sn) that constituted the surface layer on a Si(111) substrate by comparing relative short-range forces. We show that the four unique adatom types on the Si(111)-7 × 7 surface can be clearly distinguished by their force profiles. However, the ratio between attractive forces over different adatom species is highly dependent upon the tip state. By characterizing the tip with a CO molecule adsorbed on a Cu surface, a method we refer to as CO Front atom Identification (COFI), we can perform force spectroscopy with a well-defined tip apex.

While the 7 × 7 reconstruction of the Si(111) surface has a complex structure (shown in Figure 1a), it is also ideally suited for this investigation because the topmost adatom layer contains four inequivalent adatom types: the corner and center adatoms on the faulted and unfaulted half of the unit cell (CoF, CeF, CeU, CoU). The adatoms are also uniquely bound to their neighboring atoms in the lower layer. We can model the effect of this on force spectroscopy, as shown in Figure 1b, by using the Stillinger–Weber potential[4] to describe the interaction between tip and sample atoms. In this framework, we would expect a difference of approximately 50 pN between the different types of adatoms in the attractive regime.

After the Si(111)-7 × 7 surface was atomically resolved by NC-AFM,[5] differences in imaging adatoms on faulted and unfaulted halves with large amplitude NC-AFM were

* Address correspondence to franz.giessibl@ur.de.

Received for review June 19, 2013 and accepted July 10, 2013.

Published online July 10, 2013
10.1021/nn403106v

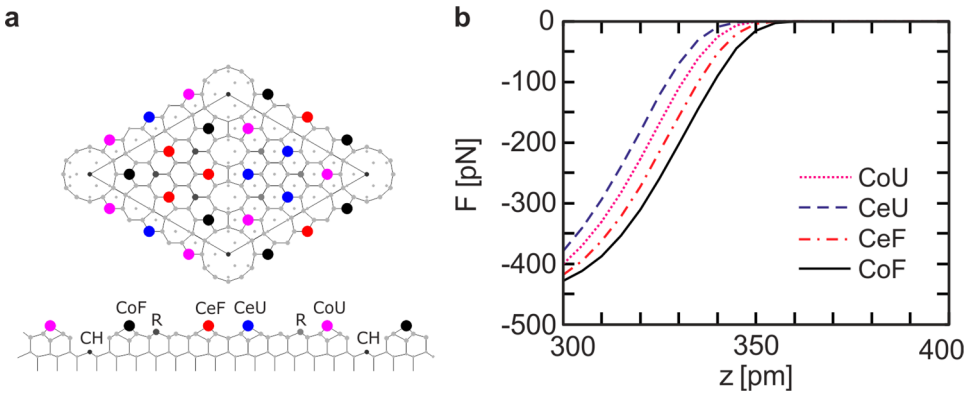

Figure 1. (a) DAS model of the Si(111)-7 × 7 surface. The top layer of the unit cell consists of 12 adatoms arranged in a faulted (F) and an unfaulted (U) half. The inequivalent adatom sites are categorized in corner adatoms (CoF, CoU) surrounding the corner hole (CH) and the center adatoms (CeF, CeU). (b) Calculated force spectra of a Si single-atom tip interacting with each adatom species *via* a Stillinger−Weber potential[4] using atomic positions determined by *ab initio* calculations.[28]

reported.[6−8] They all indicate that the interaction strength over inequivalent adatoms sites varies due to differences in electrostatic and chemical interaction. A theoretical study of the interaction between a Si tip and a Si(111)-5 × 5 surface was presented by Perez *et al.*[9] In this work, the authors pointed out that, close to the sample, only the variation of the chemical bonding force is strong enough to achieve atomic resolution. After the first spectroscopic measurements on Si(111)-7 × 7 showing differences in chemical bonding between different adatom sites,[2] Lantz *et al.* reported a weak contrast mechanism due to short-range electrostatic interaction with an oxidized Silicon tip.[10]

The COFI technique, in which we use a Δf image taken at close tip−sample distance to evaluate the angular orientation of the tip apex, came about from experiments exploring subatomic features in NC-AFM images. On Si(111)-7 × 7, the angular dependence of bonding forces was initially observed with NC-AFM between a Si tip with a Si adatom.[11,12] These subatomic features were due to the directional dependence of the covalent bonds between tip and surface atoms. In ref 13, we showed how the angular bonding symmetry of tungsten tips can be measured over a CO molecule adsorbed on a Cu(111) substrate. The data could be described by a semiempirical model assuming an attractive component along the next-to-nearest-neighbor ⟨001⟩ directions. In this model, the W atom is described as multipole with an increased electron density pointing in the eight nearest-neighbor ⟨111⟩ directions. Because of its lone pair, the CO is not expected to evolve an electronic overlap with W valence electrons to form a covalent bond. Therefore, the interaction is assumed to be electrostatic. We focused our analysis on three high-symmetry orientations. The analysis of the data led to the assignment that a W[001] tip has a single minimum in the force signal, a W[011] tip has 2-fold symmetric minima, and a W[111] tip exhibits 3-fold symmetric minima.

In this article, we use COFI to characterize the interaction between the Si(111)-7 × 7 adatoms and different W tips with defined angular bonding symmetries. Additionally, we performed high-precision force spectroscopy with Si terminated tips. A clear difference is resolved in the short-range force for all four inequivalent adatoms on the Si(111)-7 × 7 surface. We also performed measurements with tips prepared with standard methods, that is, tips that were poked into the Si surface until atomic resolution was obtained. We see differences in the spectra depending on the tip state and the various species of adatoms.

RESULTS AND DISCUSSION

A measurement cycle for the W tips consists of three steps: the initial tip preparation and characterization with COFI, the actual spectroscopic measurements on Si(111)-7 × 7, and the final COFI. To perform the COFI, we scanned the clean tungsten tip over a CO molecule adsorbed on a Cu(111) sample showing the angular bonding symmetry of the front atom. By a soft poking event, the configuration of the apex was changed without contaminating the apex with Cu atoms (details are described in ref 13). Subsequently, the angular bonding symmetry of the tip was again characterized over the CO. This procedure was repeated until the desired bonding symmetry was obtained. After the tip preparation and characterization, the Cu(111) sample was replaced by the Si(111)-7 × 7 sample and the spectroscopic measurements were performed. After the spectroscopic measurements, the tip was again characterized over a CO molecule adsorbed on the Cu(111) sample.

In Figure 2, two measurement cycles are shown for the W tips. Figure 2a,e shows Δf images of the bonding symmetry of a W front atom over a CO molecule. The COFI images reflect the bonding symmetry of a W[001] tip in Figure 2a and a W[111] tip in Figure 2d before the spectroscopic measurement on Si(111)-7 × 7. Figure 2b,e shows the images of a CoF adatom on Si(111)-7 × 7 taken with the W[001] and the W[111] tip. In Figure 2c,f, the COFI images of the same W[001] and W[111] tips are shown after the measurement on Si(111)-7 × 7.

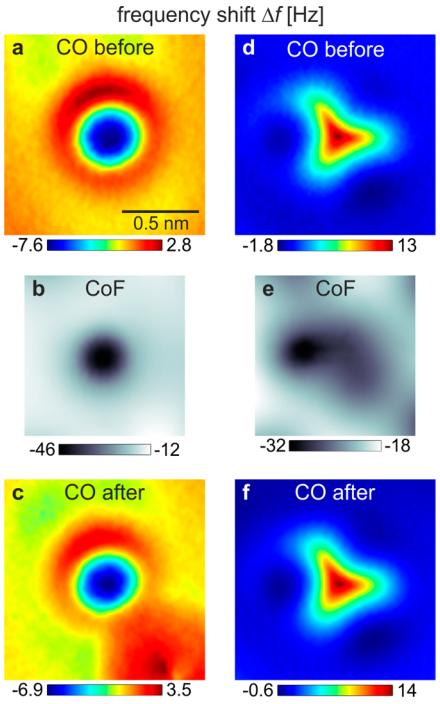

Figure 2. Carbon-oxide-front-atom-identification of the tungsten tips showing the angular bonding symmetry. The left column displays Δf images taken with the same W[100] tip (a) over a CO molecule prior measurement, (b) over a CoF adatom on Si, and (c) over a CO molecule after measurement. The right column (d−f) shows equivalent images for a W[111] tip. All images are in the same scale given in panel a.

In Figure 2c, in the lower right corner a repulsive circular area is visible. This is most likely due to a CO molecule adsorbed to the side of the apex, as the repulsive pattern corresponds to a CO/CO interaction. The CO got there presumably by diffusion due to the rise in temperature during sample transfer from Cu to Si or by adsorption from the gas phase during replacing the Cu sample by a Si sample. From the COFI images before and after the spectroscopic measurement, it is evident that the orientation and termination of the W tip apex atoms have not changed during sample transfer and measurement on the Si surface. Thus, it is possible to exchange the sample and measure on a reactive surface such as Si(111)-7 × 7 without contaminating the apex with the reactive Si atoms.

A comparison of Figure 2a with Figure 2d and Figure 2b with Figure 2e leads to the conclusion that the bonding mechanism between W and Si in the observed tip−sample distance is qualitatively similar to the interaction of W and CO on Cu. The image of the CoF probed with the W[001] tip has one pronounced minimum, whereas the image taken with the W[111] tip exhibits three spread out minima at approximately the 1:30, 4:30, and 9:00 o'clock position. However, there is no distinct repulsive contribution in the case of Si, in contrast to the interaction with the CO on Cu. If the dangling bond would covalently bind to the W atom, we would expect one pronounced minimum for the W[111] tip and four spread minima for the W[001] tip according to the bonding direction of W (see refs 14−16). While the force minima in Figure 2e are also approximately in the 1:30, 4:30, and 9:00 o'clock positions, we note that the relative depths are different. For CO/Cu (Figure 2d,f), the 4:30 o'clock position is deepest, while for Si (Figure 2e), the 9 o'clock position is deepest. This can be explained by a slightly different angle of the sample mount. Also, the distance of the three minima is larger in Figure 2d,f than in Figure 2e. We explain this by the weak lateral stiffness of CO: it is easy to bend CO laterally, as has been observed in previous studies.[13,17] See Supporting Information for more details.

Figure 3 shows Δf images of the Si(111)-7 × 7 unit cell probed with four different tips, namely, the W[001] tip in Figure 3a, the W[111] tip in Figure 3b, Si tip 1 in Figure 3c, and Si tip 2 in Figure 3d. The W tips discussed above show the same footprint for all adatoms. The bright spots in Figure 3a are a result of the influence of the laterally attached CO molecule to the W[001] tip. The minor influence of this attached CO is discussed in the Supporting Information. The orientation of the Si tips is *a priori* unknown. However, as the dangling bonds of the adatoms are symmetric with respect to the surface normal, the angular dependence must originate from the orbital structure of the tip due to the convolution of tip and sample states, similar to that recently reported by Chiutu *et al.*[18] The adatoms probed with Si tip 1 are symmetric with respect to rotations around the surface normal. This footprint could originate from a Si[111] tip with one dangling bond pointing toward the Si(111)-7 × 7 surface.[12] Si tip 2 has a more complex structure that is not aligned in a high symmetry direction.

In all Δf images, a site dependent contrast over the inequivalent adatoms is discernible that varies with tip material and tip orientation. Figure 4 shows the short-range force spectra $F_{sr}(z)$ over the inequivalent adatom sites for all four tips. (Δf spectra are included in the Supporting Information.) A branching into the inequivalent adatom sites occurs close to the surface from 100 to 0 pm. However, the run of the spectra and the order in the absolute attractive force are not identical for all tips.

Although the shape of the spectra above adatoms differs significantly for the W[001] tip and the W[111] tip, the according spectra coincide very well assuming a shift in the closest approach of 20 pm for the W[111] tip. The order in the absolute attractive force near the closest approach is CoF > CeF > CeU > CoU. For the W[001] tip, the CoF is with almost −500 pN twice as attractive as the group of CeF, CeU ,and CoU with −200 to −250 pN. These force values are in accordance with the observation that no covalent bond has been formed jet. For example, in ref 19, the authors found that the covalent bond of a W[100] apex atom and a

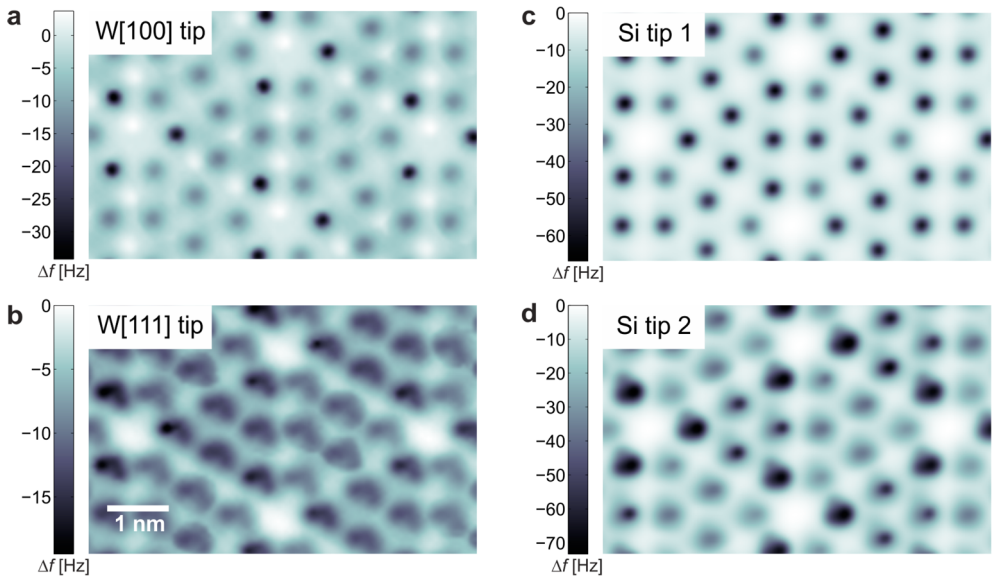

Figure 3. Δf images of the Si(111)-7 × 7 surface taken with four different tips at the closest approach: (a) W[001] tip, (b) W[111] tip, (c) Si tip 1, and (d) Si tip 2. The images show the footprints of the tips and differences among the inequivalent adatom sites.

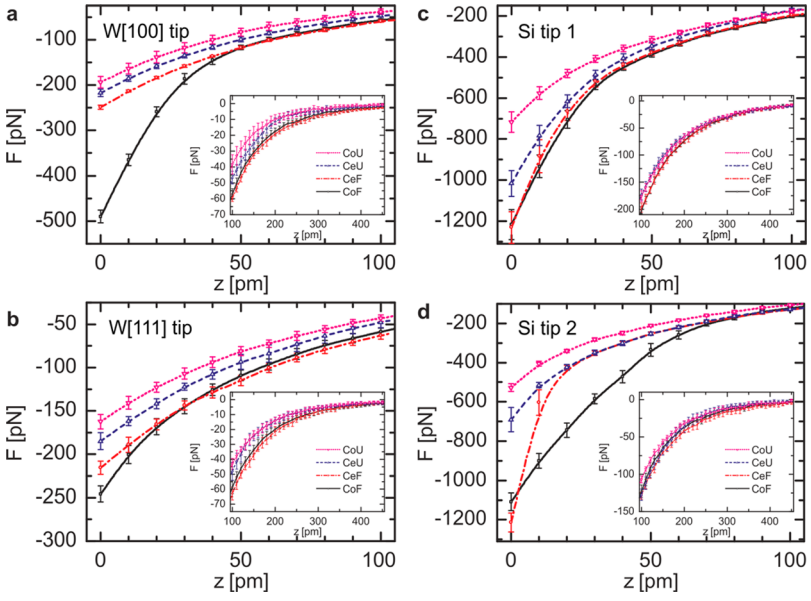

Figure 4. (Color online) Short range force spectra over CoU, CeU, CeF, and CoF adatom for the W[100] tip (a), W[111] tip (b), the Si tip 1 (c) and the Si tip 2 (d). The spectra of the first 100 pm from closest approach (arbitrarily set to 0 pm) show the splitting in the inequivalent adatom sites. The insets display the spectra from 100 pm onward splitting in the faulted and unfaulted halves for the W tips and the Si tip 1. The error bars correspond to the standard deviation over equivalent adatom sites.

Si corner adatom sets in at tip−sample distance of 500−475 pm corresponding to a short-range force of −400 to −700 pN (see Figure 2 in ref 19).

The attractive forces measured with the Si tips are much stronger compared to the W tips. This is expected for the Si tips forming a covalent bond with the Si(111)-7 × 7 adatoms. The order in the absolute attractive force for Si tip 1 is CoF ≈ CeF > CeU > CoU. For Si tip 2, the attractive forces over the inequivalent adatom sites branch in two stages. From 100 to 20 pm, only the CoU and CoF split up. In this regime, the order in the absolute attractive force is given by CoF > CeF ≈ CeU > CoU. Closer to the surface, from 20 to 0 pm, the order in the absolute attractive force approaches CeF > CoF > CeU > CoU. Thus, for the Si tips, the short-range forces are not similar over the different adatoms, even though the maximum attractive force is comparable for both tips. The insets in Figure 4 show the short-range spectra in a range from 100 to 450 pm. In this regime, the main contrast difference in the image is between faulted and unfaulted halves, which is observable for the W tips and Si tip 1. With the Si tip 2, a clear distinction of the unit cell halves is not possible in this range. It is noted that the spectra do not extend to the local force minima, because

entering this distance range endangers the integrity of the tip, and would defeat the intended demand of the experiments shown here: force spectroscopy using tips that are characterized by COFI before *and* after taking the spectra, using only those spectra where the tip did not suffer any changes during acquiring the spectroscopy curve.

It is noteworthy that the CoU followed by the CeU is the least attractive adatom for all four tips. This does not match, for example, the results of our Stillinger–Weber model shown in Figure 1b, or the geometric positions of the adatoms as measured by LEED[20] or calculated by DFT.[21] The *z*-position of the CoU is higher than the *z*-position of the CeU, which would lead to a stronger attraction in the range with a positive slope of F_{sr}. Also, a diminished van der Waals background near the corner hole cannot account for the differences, as it is shown in the Supporting Information. A simulation of the van der Waals force over the Si(111)-7 × 7 surface leads to a site-specific contrast in the order of a few 100 fN. We propose that the force contrast among the four adatom types is due to variances in subsurface bonding and possibly due to the differences in local charge at the four adatom types.

CONCLUSIONS

We demonstrated the discrimination of all four adatom sites on Si(111)-7 × 7 by high-precision force spectroscopy with four different tip states. This extends the possibility of chemical identification to the identification of different bonding sites of one atom species. The differences between the inequivalent adatom sites partly depend on the state of the tip and on the tip material, but also on the local environment of the adatom. In images that resolve the angular bonding symmetry, it is important to take the position of the spectra over the adatoms into account. Therefore, a thorough understanding of the angular bonding symmetry of the front atom is necessary, as it can be achieved by the COFI method presented in this Article. Furthermore, this information is valuable for first-principle calculations of the interaction in NC-AFM, as assumptions about the apex orientation are not necessary. We note that the use of precisely characterized tips that are used to perform absolute force measurements on well-defined surface atoms like the four different adatoms in Si(111)-7 × 7 might enable a traceable calibration of forces and force gradients at the atomic scale, an important issue for metrology on the nanoscale.

METHODS

The experiments were performed in a commercial UHV low temperature AFM/STM (Omicron LT-QPlus SPM, Omicron Nano-Technology GmbH, D-65232 Taunusstein Germany) operating at 4.4 K in frequency modulation mode with a tuning fork sensor in qPlus configuration.[22] We used two sensors for the measurements with a spring constant of k = 1800 N/m. The first sensor was equipped with an etched W tip that was cleaned *in situ* by field evaporation. The resonance frequency was f_0 = 26645.8 Hz and the quality factor Q = 422670. The second sensor had a resonance frequency of f_0 = 27045.2 Hz and a quality factor of Q = 40353. The W tip of this sensor was also cleaned by field evaporation. All measurements were done with an oscillation amplitude of A = 50 pm.

We used a boron p-doped silicon sample in (111) orientation with a resistivity of 0.01–0.02 Ω cm. The silicon sample was prepared with the standard method of repeated cycles of flashing and annealing. After preparation, the sample was directly transferred into the microscope and kept at the measurement temperature of 4.4 K.

When transferring from Si to Cu or back, we record a maximum temperature of 20 K in the microscope head.

We took constant height Δf images in a range of 500 pm in 10 pm steps starting close to the surface. The images were taken at 0 V bias voltage to prevent the effects of the phantom force.[23,24] The phantom force is an apparently repulsive force that can obscure the chemical atomic contrast of an AFM image when a tunneling current is present. For analysis, we smoothed the constant height Δf images with a Gaussian filter with a spatial cutoff frequency of 20 nm^{-1}, thus, Δf was measured at an effective bandwidth of B = 1.28 Hz. The lateral drift was compensated as described in ref 25. The Δf-spectra were extracted from the constant height Δf images at the minimum of each adatom sites. The data was averaged over forward and backward scans and over equivalent adatom sites. The long-range van der Waals (vdW) and electrostatic background was measured over the corner hole and subtracted from the Δf spectra over the adatoms to obtain the short-range Δf spectra. Finally, we determined the short-range force F_{sr} using the matrix deconvolution method.[26,27]

Conflict of Interest: The authors declare no competing financial interest.

Supporting Information Available: Includes a discussion on the adsorbed CO molecule at the W[001] tip, a description of the simulation of van der Waals forces, and of the chemical interaction. This material is available free of charge *via* the Internet at http://pubs.acs.org.

Acknowledgment. Financial support from the Deutsche Forschungsgemeinschaft (Graduiertenkolleg 1570 and Sonderforschungsbereich 689) is kindly acknowledged.

REFERENCES AND NOTES

1. Barth, C.; Foster, A. S.; Henry, C. R.; Shluger, A. L. Recent Trends in Surface Characterization and Chemistry with High-Resolution Scanning Force Methods. *Adv. Mater.* **2011**, *23*, 477–501.
2. Lantz, M. A.; Hug, H. J.; Hoffmann, R.; Schendel, P. J. A.; van Kappenberger, P.; Martin, S.; Baratoff, A.; Güntherodt, H.-J. Quantitative Measurement of Short-Range Chemical Bonding Forces. *Science* **2001**, *291*, 2580–2583.
3. Sugimoto, Y.; Pou, P.; Abe, M.; Jelinek, P.; Pérez, R.; Morita, S.; Custance, O. Chemical Identification of Individual Surface Atoms by Atomic Force Microscopy. *Nature* **2007**, *446*, 64–67.
4. Stillinger, F. H.; Weber, T. A. Computer Simulation of Local Order in Condensed Phases of Silicon. *Phys. Rev. B* **1985**, *31*, 5262–5271.
5. Giessibl, F. J. Atomic Resolution of the Silicon (111)-(7 × 7) Surface by Atomic Force Microscopy. *Science* **1995**, *267*, 68–71.
6. Erlandsson, R.; Olsson, L.; Mårtensson, P. Inequivalent Atoms and Imaging Mechanisms in Ac-Mode Atomic-Force Microscopy of Si(111)7 × 7. *Phys. Rev. B* **1996**, *54*, R8309–R8312.

7. Nakagiri, N.; Suzuki, M.; Okiguchi, K.; Sugimura, H. Site Discrimination of Adatoms in Si(111)-7 × 7 by Noncontact Atomic Force Microscopy. *Surf. Sci.* **1997**, *373*, L329–L332.
8. Uchihashi, T.; Sugawara, Y.; Tsukamoto, T.; Ohta, M.; Morita, S.; Suzuki, M. Role of a Covalent Bonding Interaction in Noncontact-Mode Atomic-Force Microscopy on Si(111)7 × 7. *Phys. Rev. B* **1997**, *56*, 9834–9840.
9. Pérez, R.; Štich, I.; Payne, M.; Terakura, K. Surface-Tip Interactions in Noncontact Atomic-Force Microscopy on Reactive Surfaces: Si(111). *Phys. Rev. B* **1998**, *58*, 10835–10849.
10. Lantz, M.; Hug, H.; Hoffmann, R.; Martin, S.; Baratoff, A.; Güntherodt, H.-J. Short-Range Electrostatic Interactions in Atomic-Resolution Scanning Force Microscopy on the Si(111)7 × 7 Surface. *Phys. Rev. B* **2003**, *68*, 035324.
11. Giessibl, F. J.; Hembacher, S.; Bielefeldt, H.; Mannhart, J. Subatomic Features on the Silicon (111)-(7 × 7) Surface Observed by Atomic Force Microscopy. *Science* **2000**, *289*, 422–425.
12. Huang, M.; Čuma, M.; Liu, F. Seeing the Atomic Orbital: First-Principles Study of the Effect of Tip Termination on Atomic Force Microscopy. *Phys. Rev. Lett.* **2003**, *90*, 256101.
13. Welker, J.; Giessibl, F. J. Revealing the Angular Symmetry of Chemical Bonds by Atomic Force Microscopy. *Science* **2012**, *336*, 444–449.
14. Wright, C. A.; Solares, S. D. On Mapping Subangstrom Electron Clouds with Force Microscopy. *Nano Lett.* **2011**, *11*, 5026–5033.
15. Mattheiss, L.; Hamann, D. Electronic Structure of the Tungsten (001) Surface. *Phys. Rev. B* **1984**, *29*, 5372–5381.
16. Posternak, M.; Krakauer, H.; Freeman, A.; Koelling, D. Self-Consistent Electronic Structure of Surfaces: Surface States and Surface Resonances on W(001). *Phys. Rev. B* **1980**, *21*, 5601–5612.
17. Gross, L.; Mohn, F.; Moll, N.; Schuler, B.; Criado, A.; Guitián, E.; Peña, D.; Gourdon, A.; Meyer, G. Bond-Order Discrimination by Atomic Force Microscopy. *Science* **2012**, *337*, 1326–1329.
18. Chiutu, C.; Sweetman, A. M.; Lakin, A. J.; Stannard, A.; Jarvis, S.; Kantorovich, L.; Dunn, J. L.; Moriarty, P. Precise Orientation of a Single C_{60} Molecule on the Tip of a Scanning Probe Microscope. *Phys. Rev. Lett.* **2012**, *108*, 268302.
19. Jelínek, P.; Švec, M.; Pou, P.; Perez, R.; Cháb, V. Tip-Induced Reduction of the Resonant Tunneling Current on Semiconductor Surfaces. *Phys. Rev. Lett.* **2008**, *101*, 176101.
20. Huang, H.; Tong, S. Y.; Packard, W. E.; Webb, M. B. Atomic Geometry of Si(111) 7 × 7 by Dynamical Low-Energy Electron Diffraction. *Phys. Lett. A* **1988**, *130*, 166–170.
21. Ke, S. H.; Uda, T.; Terakura, K. Surface Topography of the Si(111)-7 × 7 Reconstruction. *Phys. Rev. B* **2000**, *62*, 15319–15322.
22. Giessibl, F. J. Atomic Resolution on Si(111)-(7 × 7) by Noncontact Atomic Force Microscopy with a Force Sensor Based on a Quartz Tuning Fork. *Appl. Phys. Lett.* **2000**, *76*, 1470–1472.
23. Weymouth, A. J.; Wutscher, T.; Welker, J.; Hofmann, T.; Giessibl, F. J. Phantom Force Induced by Tunneling Current: A Characterization on Si(111). *Phys. Rev. Lett.* **2011**, *106*, 226801.
24. Wutscher, T.; Weymouth, A. J.; Giessibl, F. J. Localization of the Phantom Force Induced by the Tunneling Current. *Phys. Rev. B* **2012**, *85*, 195426.
25. Albers, B. J.; Schwendemann, T. C.; Baykara, M. Z.; Pilet, N.; Liebmann, M.; Altman, E. I.; Schwarz, U. D. Data Acquisition and Analysis Procedures for High-Resolution Atomic Force Microscopy in Three Dimensions. *Nanotechnology* **2009**, *20*, 264002.
26. Giessibl, F. J. A Direct Method to Calculate Tip-Sample Forces from Frequency Shifts in Frequency-Modulation Atomic Force Microscopy. *Appl. Phys. Lett.* **2001**, *78*, 123–125.
27. Welker, J.; Illek, E.; Giessibl, F. J. Analysis of Force-Deconvolution Methods in Frequency-Modulation Atomic Force Microscopy. *Beilstein J. Nanotechnol.* **2012**, *3*, 238–248.
28. Brommer, K. D.; Needels, M.; Larson, B.; Joannopoulos, J. *Ab Initio* Theory of the Si (111)-(7 × 7) Surface Reconstruction: A Challenge for Massively Parallel Computation. *Phys. Rev. Lett.* **1992**, *68*, 1355–1358.